Acta Biochim Biophys Sin, 2020, 52(6), 620–630
doi: 10.1093/abbs/gmaa039
Advance Access Publication Date: 2 June 2020
Original Article

Original Article

Role and effect of vein-transplanted human umbilical cord mesenchymal stem cells in the repair of diabetic foot ulcers in rats

Rongfeng Shi[1,†], Weishuai Lian[2,3,†], Yinpeng Jin[4,†], Chuanwu Cao[2,3], Shilong Han[2,3], Xiaohu Yang[1], Suming Zhao[1], Maoquan Li[2,3,*], and Hui Zhao[1,*]

[1]Department of Interventional Radiology, Affiliated Hospital of Nantong University, Nantong 226001, China, [2]Department of Interventional & Vascular Surgery, Shanghai Tenth People's Hospital, Tongji University, School of Medicine, Shanghai 200072, China, [3]Institute of Medical Intervention Engineering, Tongji University, Shanghai 200072, China, and [4]Shanghai Public Health Clinical Center, Fudan University, Shanghai 201508, China

[†]These authors contributed equally to this work.

*Correspondence address. Tel/Fax: +86-21-66301045, E-mail: cjr.limaoquan1965@vip.163.com (M.L.) / Tel/Fax: +86-513-85052201; E-mail: zhaohui8868@sina.com (H.Z.)

Received 4 November 2019; Editorial Decision 20 January 2020

Abstract

Diabetic foot ulcer (DFU) is one of diabetic complications, which is frequently present and tormented in diabetes mellitus. Most multipotent mesenchymal stromal cells (MSCs) are capable of immune evasion, providing an allogeneic, ready-to-use, cell product option for therapeutic applications. The beneficial effect of MSCs for the treatment of a variety of traumatic injuries, such as open wounds, has been extensively explored. In this study, a rat DFU model was used to simulate the pathophysiology of clinical patients and to investigate the localization of human umbilical cord mesenchymal stem cells (hUC-MSCs) after intravenous transplantation and its role in DFU healing, so as to evaluate the potential of hUC-MSCs in the treatment of DFU. The diabetic rat model was established by streptozotocin injection, which was used to create full-thickness foot dorsal skin wounds to mimic DFU by a 6-mm skin biopsy punch and a Westcott scissor. The hUC-MSCs were transplanted through femoral vein, and the ulcer cicatrization situation and the fate of hUC-MSCs were evaluated. Our data suggest that intravenously transplantated hUC-MSCs have the ability to migrate and locate to the wound tissue and are helpful to wound healing in DFU rats, partly by regulating inflammation, trans-differentiation and providing growth factors that promote angiogenesis, cell proliferation and collagen deposition. Herein, we demonstrate that hUC-MSC transplantation is able to accelerate DFU healing in rats and transplantation of exogenous stem cells may be a potential strategy for clinical application in DFUs.

Key words: human umbilical cord mesenchymal stem cells, diabetic foot ulcer, tissue repair

Introduction

Diabetes mellitus (DM) is a metabolic syndrome characterized by the prevalence of hyperglycemia, resulting from a deficiency of insulin secretion or its inability to properly perform its functions. Despite increased prevention efforts and improved understanding of the situation, the prevalence rate has continued to rise in recent decades and shifted to developing countries [1]. DM complications have a degenerative character and usually occur in a time interval of 5 to 10 years after disease onset. Tissue loss complications in diabetic patients have been identified as the main cause of hospitalization and

non-traumatic lower extremity amputation [2]. Diabetic foot ulcer (DFU) is one of the complications, which is correlated with failure of healing, longer length of inpatient stay, and increased mortality [3]. DFU is an outcome of complicated amalgam of various risk factors such as peripheral neuropathy, peripheral vascular disease, foot deformities, arterial insufficiency, trauma and impaired resistance to infection, with the persistent hyperglycemia state, which make the DFU difficult to heal than normal wounds [4]. Due to the limited efficacy of traditional treatment methods, DFU treatment remains an important clinical challenge and new methods to promote the healing of diabetic foot disease are constantly studied to reduce morbidity and mortality.

Mesenchymal stem cells (MSCs) are considered as potential candidates for a variety of therapeutic applications, such as immune disorders, including graft-versus-host disease and systemic lupus erythematosus, bone and cartilage regeneration, nervous system diseases and chronic ulcerative lesions [5–9]. Stem cells are one kind of undifferentiated cells that can be extensively expanded *in vitro* [10]. MSCs are adult stem cells with unique characteristics including long-term *ex vivo* proliferation, multilineage differentiation potential, and immunomodulatory properties [11]. Bone marrow-derived mesenchymal stem cells (BMSCs) are an important source of adult stem cells. They have been extensively studied and confirmed to play an important role in reconstructing skin and promoting wound healing [12]. Nevertheless, the harvesting of BMSCs is invasive and it is necessary to explore other substitute stem cells for practical application. Umbilical cord mesenchymal stem cells (UC-MSCs) may be a good choice. They are similar to BMSCs in their characteristics, including cell surface markers, gene expression profiles, immunosuppressive properties and differentiation ability [13]. Compared with other original MSCs, the advantages of UC-MSCs are short amplification time, high proliferation rate and higher safety [14]. In addition, the stem cells harvested from the umbilical cord are abundant at the cell source, easy to acquire, without any ethical difficulties, and with little immunogenicity [15]. Although UC-MSCs have been reported to have multiple tissue repair effects, few studies have been conducted on UC-MSCs for DFU treatment.

In this study, the hUC-MSCs were transplanted via the left femoral vein in the DFU rats, and their effects on wound healing compared with the control group were detected. We also traced the mobilization and localization of transplanted hUC-MSCs to DFUs with the lentivirus expressing ZsGreen. In addition, inflammatory factors and growth factors in foot ulcer tissue were analyzed to further explore their potential mechanisms in wound healing. We found that hUC-MSCs have the ability to detect ulcer tissue and accelerate ulcer healing through paracrine and trans-differentiation, which provides important information for their potential clinical application.

Materials and Methods

Isolation and culture of hUC-MSCs

All human umbilical cords were obtained from the Department of Obstetrics and Gynecology, Affiliated Hospital of Nantong University. Written informed consent was obtained from the patients' families in accordance with procedures approved by the ethics committee at the Affiliated Hospital of Nantong University. The umbilical cords were kept at 4°C and transported to the laboratory, washed three times by sterile phosphate-buffered saline (PBS) with 1% penicillin/streptomycin (Sigma-Aldrich, St Louis, USA). After removal of all the vessels, the remaining tissues were chopped with sterile operation scissors and digested with 0.5% collagenase type II (Sigma-Aldrich) at 37°C for 8 h. The samples were neutralized with isometric culture media and centrifuged at 250 *g* for 5 min. The sediments were resuspended and cultured in Dulbecco's modified Eagle's medium/F12 (DMEM/F12) medium (Gibco, Gaithersburg, USA) supplemented with 10% fetal bovine serum (FBS; Gibco), 100 U/ml penicillin, 100 μg/ml streptomycin, and 2 mM L-glutamine (Sigma-Aldrich) in a humidified incubator (Thermo Fisher Scientific, Waltham, USA) supplemented with 5% CO_2, and the medium was changed every other day. The primary hUC-MSCs were routinely examined under a phase-contrast inverted microscope (Leica DMR 3000; Leica Microsystem, Wetzlar, Germany). For continuous cell culture of hUC-MSCs, the adherent hUC-MSCs at 80% confluence were washed with PBS and transferred into a petri dish containing culture medium with 0.2% trypsin-EDTA (Gibco) at 37°C for 2 min. The cell suspension was transferred into a 15-ml tube and centrifuged at 250 *g* for 5 min, and the supernatant was removed and the pallet of hUC-MSCs was then resuspended in the 15-ml tube of culture medium, and 6×10^3 cells/cm^2 of hUC-MSCs were plated onto petri dishes for continuous cell culture. Cells were used for the subsequent study after 2–3 passages.

Identification of hUC-MSC surface markers

Immunofluorescent assay and flow cytometry were employed to detect the phenotypes of hUC-MSCs. Passage 3 hUC-MSCs were seeded into a six-well plate and cultured overnight, fixed by 4% paraformaldehyde for 1 h, and incubated with CD29-FITC, CD44-PE, CD90-FITC, CD105-PE, CD34-FITC, and CD133-PE anti-human antibodies (0.5 μl/well; Abcam, Cambridge, UK) for 1 h at room temperature. After being rinsed three times with PBS, cells were stained with DAPI solution. The fluorescence of hUC-MSCs was detected with the Leica DMR 3000 microscope.

For flow cytometric analysis, passage 3 hUC-MSCs were used to prepare single-cell suspension, and 2 μl of CD29-FITC, CD44-PE, CD90-FITC, CD105-PE, CD34-FITC, and CD133-PE anti-human antibodies were added subsequently into the suspension. These cell suspensions were incubated for 30 min on ice in the dark, and then observed with a BD FACSAria III flow cytometer (BD Biosciences, Franklin Lakes, USA).

Animal care and models for DFUs

Specific pathogen-free adult female Sprague-Dawley rats (150–200 g; grade: clean; license: SCXK 2013-0005) at the age of 4 to 6 weeks were provided by SLAC Laboratory Animal Co., Ltd (Shanghai, China) and used to establish DFU model. The rats were maintained on a 12-hour light cycle in the animal facility of the Animal Unit of Nantong University. The rats were fasted for solids and liquids for 8 h and injected intraperitoneally once with 100 mg/kg of STZ (Sigma-Aldrich) to induce diabetes. After that, free access to fat food and water was given, and the blood glucose was checked every other day. One week after injection with STZ, the following criteria were employed to select successful DFU model rats: (i) blood glucose over 16.7 mM and (ii) blood glucose levels controlled (16.7–33.3 mM) by 6–18 units/day of insulin (Wan-Bang Biochemical Medicine Co., Ltd, Xuzhou, China). After 8 weeks of fat food feeding, the DFU model rats of high level blood glucose were subject to following treatment: diabetes rats were anesthetized with intramuscular injection of ketamine (50 mg/kg), and a single round full-thickness skin wound

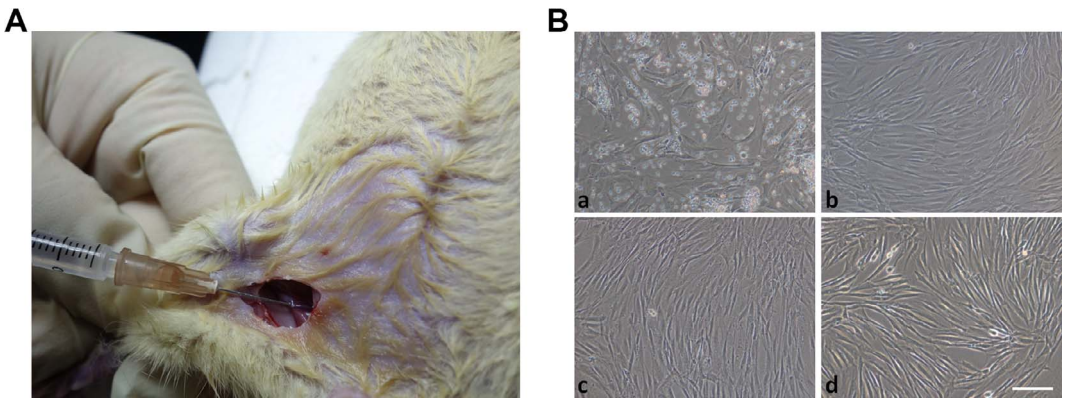

Figure 1. Schematic diagram of the hUC-MSC culture and injection (A) The models of DFU rats were injected with 1 ml hUC-MSCs or PBS via contralateral femoral vein each. (B) Representative microphotographs of primary (a), passage 1 (b), passage 2 (c), and passage 3 (d) hUC-MSCs. After several passages, the morphology of expanded hUC-MSCs appeared to be shuttle-shaped, became uniform, showing better size and refraction under the microscope. Scale bar, 100 μm.

was created in the dorsum of the foot by a disposable 6-mm skin biopsy punch and Westcott scissor. All the experiments with animals were performed in Laboratory Animal Center of Nantong University, and all animal experiments were conducted in accordance with the standard operating procedures for laboratory animal center of Nantong University approved by the Lab Animal Ethical Committee of Nantong University.

Transplantation of hUC-MSCs to DFU rats

A total of 30 DFU model rats were successfully duplicated and randomly divided into two groups: the treatment group and the control group. The left femoral vein was found with blunt dissection, and 5×10^6 hUC-MSCs suspended in 1 ml PBS was injected into each rat in the treatment group, and each rat in the control group was injected with equal volume of PBS (Fig. 1A). Then local hemostasis and wound suturation were performed. At Day 3 (D3), 8 (D8), and 16 (D16) after treatment, five rats in each group were randomly selected and sacrificed, and the feet with diabetic ulcer were harvested. The feet were divided into two equal parts vertically along the center line of the ulceration with scissor. Half of each foot was stored immediately at −80°C for the detection of cytokines by proteome profiler array and enzyme-linked immunosorbent assay (ELISA), and the other half was fixed with 4% phosphate-buffered paraformaldehyde for hematoxylin and eosin (H&E) staining, Masson's trichrome staining and immunohistochemical analysis. The blood glucose was checked daily and well-controlled at 16.7 and 33.3 mM by 6 ~ 18 units/day of insulin during the whole process.

Measurement of DFU area

At D3, D8, and D16 post-treatment, parfocal digital photographs with a ruler were taken for each foot with a DSC-HX50 digital camera (Sony, Tokyo, Japan) before the harvest. The ulcer area in each foot was measured from the pictures taken at each time point using Image-Pro Plus 6.0 image analysis software.

Histological and immunohistochemical assessment of DFU healing

To detect the re-epithelialization/granulation tissue formation and collagen deposition, H&E staining and Masson's trichrome staining were employed. The DFU tissues at D16 post-treatment were collected from rat feet in the control and hUC-MSC treatment groups, fixed with 4% phosphate-buffered paraformaldehyde, embedded in paraffin, and sectioned at 4.0 μm. The sections were dehydrated with successive concentrations of ethanol and washed twice with distilled water, followed by H&E staining and Masson's trichrome staining according to the protocols of the manufacturer (Cyagen Biosciences Inc., Santa Clara, USA).

The microvessel density in the DFU tissues at D16 was analyzed by immunohistochemical analysis using rat anti-CD31 primary antibody. The sections of the samples were blocked with 3% normal goat serum/0.3% Triton X-100/0.1% BSA (Sigma-Aldrich) in PBS. The sections were then incubated overnight at 4°C with the primary antibody against CD31 (1:200 dilution, sc-53526; Santa Cruz Biotech, Santa Cruz, USA), followed by incubation with horseradish peroxidase-conjugated goat anti-mouse IgG secondary antibody (1:500 dilution, ab205719; Abcam) for 60 min at room temperature. After hematoxylin staining, tissue sections were washed again and then dehydrated with ethanol, treated with dimethylbenzene, and sealed for microscopic analysis. And the status of cell apoptosis and proliferation in the DFU tissues were detected by using the terminal deoxynucleotidyl transferase dUTP nick end labeling (TUNEL) assay kit (ab66110; Abcam) and Ki-67 staining (ab15580; Abcam) according to the product instruction manuals, respectively. All the histological sections were observed under the Leica DMR 3000 microscope and analyzed with Image-Pro Plus 6.0 image analysis software across five nonconsecutive tissue sections for each wound by two blinded experienced investigators.

Detection of cytokines in DFU tissues

The cytokines in DFU tissues were detected by ELISA and proteome profiler array. The DFU tissues were washed with sterile PBS and cut into smaller pieces. Total protein was extracted, centrifuged and resuspended into sample application buffer containing a protease inhibitor cocktail (Promega, Madison, USA). The contents of VEGF, bFGF and FGF in DFU tissues at D3, D8, and D16 post-treatment were measured using the ELISA kits (Shanghai ExCell Biology, Inc., Shanghai, China) according to the product instruction manuals. The optical density of each well was determined with a spectrophotometer (Labomed, Los Angeles, USA) at 450 nm after substrate solution

of hydrogen peroxide was added, and the concentrations of cytokines were calculated. The levels of inflammatory factors and chemokines in DFU tissues at D3 post-treatment were detected with the proteome profiler array (R&D Systems, Minneapolis, USA) according to the product instruction manuals. The pixel densities on developed X-ray films were collected and analyzed using Image-Pro Plus 6.0 image analysis software.

Labeling of hUC-MSCs by ZsGreen

Preparation of labeled hUC-MSCs by ZsGreen was performed as described previously [16]. Briefly, the pLVX-ZsGreen1-N1 plasmid and packaging plasmids that include pGag/Pol, pRev, and pVSV-G (Invitrogen) were co-transfected into HEK293T cells (Kebo Bio., Shanghai, China) to package virus. After 48 and 72 h transfection, the vector-containing supernatants were harvested and then used to infect the passage 2 hUC-MSCs at 70% cell confluence. Three days after transfection, the infection efficiency was detected with an IX71 fluorescence microscope (Olympus, Tokyo, Japan) and the cells were cultured successively to passage 3 in a 37°C humidified incubator supplemented with 5% CO_2, and the medium was changed every other day.

Tracing of transplanted hUC-MSCs in DFU tissues

Twenty DFU model rats were duplicated and injected with 5×10^6 hUC-MSCs via the femoral vein as mentioned above. At 24 h, D3, D8 and D16 after transplantation, the rats were randomly selected and sacrificed, and the feet with diabetic ulcers were harvested (5 each time point). The DFU tissues were collected and embedded with OCT and stored at −80°C for fluorescent immunostaining. And 4-μm longitudinal sections from the samples were cut in a cryostat and thaw mounted onto polylysine-coated slides. The sections were rinsed three times with PBS and stained with DAPI solution (1 mg/ml). The histological sections were observed under the Leica DMR 3000 microscope and analyzed with Image-Pro Plus 6.0 image analysis software across five nonconsecutive tissue sections for each wound by two blinded experienced investigators.

To explore the differentiation of the hUC-MSCs in DFU tissues, the sections at each time point were then also incubated overnight at 4°C with the primary antibody against CD31 (1:200 dilution) or against pan-cytokeratin (1:200 dilution, sc-58826; Santa Cruz), followed by incubation with Alexa Fluor® 647-conjugated goat anti-mouse IgG secondary antibody (1:500 dilution, ab150115; Abcam) for 60 min at room temperature. These sections were also rinsed three times with PBS and stained DAPI solution (1 mg/ml). Finally, the sections were examined and photographed with the Leica DMR 3000 microscope.

Statistical analysis

Results were expressed as the mean ± SD of three independent experiments. Statistical analysis was performed using GraphPad Prism 5.0 software (GraphPad Software, La Jolla, USA). Differences between experimental groups were assessed by one-way analysis of variance followed by Dunnett's test. For all statistical analyses, P values <0.05 were considered to be statistical significance.

Results

Culture and characterization of hUC-MSCs

The morphology of expanded hUC-MSCs appeared to be shuttle-shaped and fibroblast-like. There were some red blood cells in the primary culture. After three passages, the hUC-MSC population became uniform, showing a layer of adherent cells with better size and refraction under the microscope (Fig. 1B). Immunofluorescent assay and flow cytometry analysis were employed to characterize the phenotype of passage 3 hUC-MSCs. Until now, no specific marker was found in hUC-MSCs, and we used the general phenotype for MSCs. The data revealed that CD29, CD44, CD90, and CD105 were highly expressed, whereas the cells expressed minimal levels of CD34, CD36 and CD133 (Fig. 2A). The results of flow cytometry analysis were consistent with those of immunofluorescence analysis, over 95% cells expressed CD29 (99.9%), CD44 (98.0%), CD90 (97.8%), and CD105 (99.9%), but all cells were almost negative for CD34, CD36 and CD133 (<5.0%; Fig. 2B). Because of the strong proliferation capacity, we obtained larger quantity and more purified hUC-MSCs after continuous cell culture.

Ulceration healing after hUC-MSC transplantation

There were no obvious adverse reactions and transplant rejection in the treatment group and the control group during 16 days of treatment. Figure 3 showed the representative ulcer images from the two groups at D3, D8 and D16 after treatment, the wound closure rate at relevant time points, and the level of blood glucose during the treatment. At D3 after treatment, there was no significant difference of the open wound size between the control group and the treatment group (38.6 ± 3.5 mm^2 versus 38.3 ± 2.3 mm^2, $P > 0.05$). Redness and swelling could be detected in the ulcers, although crustations were formed, the mean area of the foot ulcers were a little enlarged in both two groups probably because of the inflammatory reaction. At D8, the mean size of wound was significantly reduced with formation of black scabs and alleviation of the inflammatory responses in the treatment group, and the rate of wound closing in the treatment group ($45.1\% \pm 1.8\%$) was significantly higher than that in the control group ($26.7\% \pm 2.1\%$) with the area of 28.3 ± 2.5 mm^2 in the control group versus 21.2 ± 1.3 mm^2 in the treatment group ($P < 0.05$). Furthermore, the ulcers were significantly smaller in the group that received hUC-MSCs, when compared with those in the control group at D16, and the hUC-MSCs almost induced a wound closure of 90% with the area of 26.3 ± 2.4 mm^2 in the control group versus 3.8 ± 0.3 mm^2 in the treatment group ($P < 0.01$). Blood glucose levels in diabetic rats were consistently higher than 16.7 mM in both treatment group and control group, and there was no significant difference between the two groups during the whole experimental process, with blood glucose of 27.6 ± 2.5 mM in the control group versus 29.1 ± 3.1 mM in the treatment group ($P > 0.05$). These results suggested that vein transplantation of hUC-MSCs accelerated the ulceration healing but had no distinct therapeutic effect on blood glucose in diabetic rats.

Histological assessment of ulceration healing

Histological analysis of the ulceration tissues was performed to further evaluate the details of wound healing. H&E staining of skin sections from the DFUs at D16 after treatment showed closely complete re-epithelialization and thick granulation tissue in the treatment group, whereas not fully re-epithelialized and thinner granulation tissue in the control group (Fig. 4A). The thickness of granulation tissue in the treatment group was 293 ± 26 μm, which was significantly thicker compared with that in the control group (195 ± 18 μm, $P < 0.05$). The DFUs treated with hUC-MSCs showed greater tissue regeneration and fewer infiltrating inflammatory cells

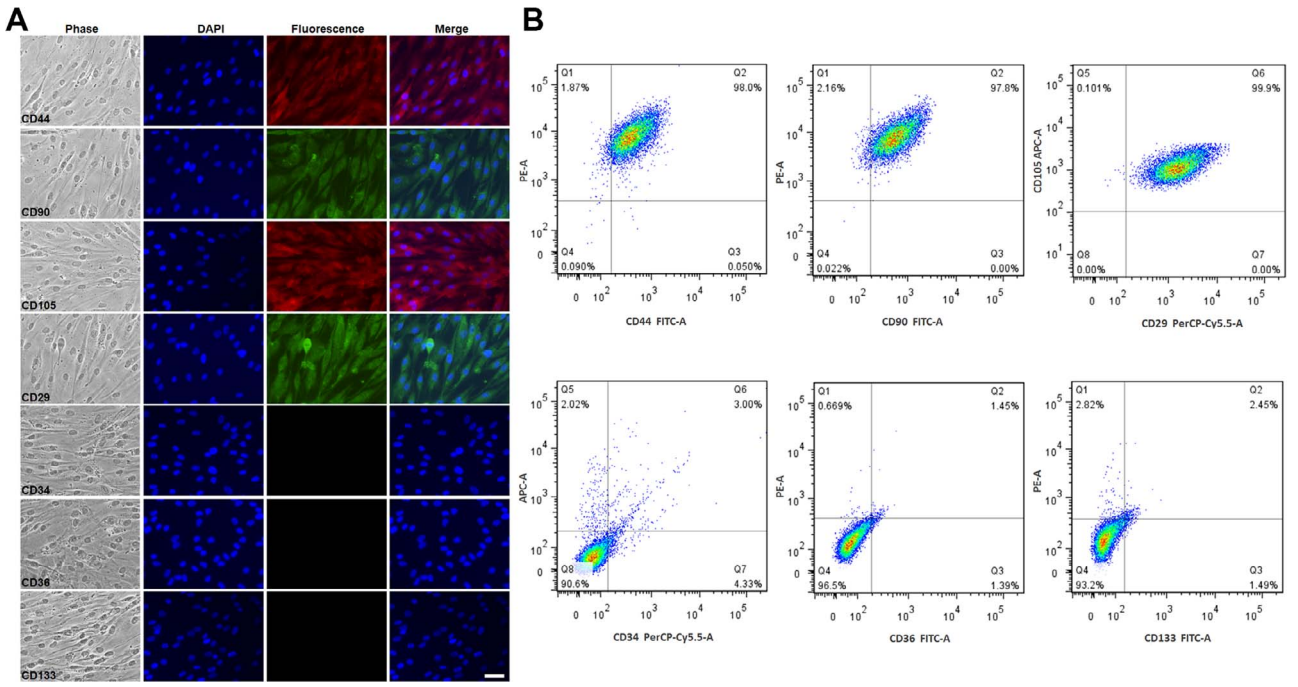

Figure 2. Characterization of passage 3 hUC-MSCs (A) Immunofluorescent assay indicated that hUC-MSCs were positive for cell surface markers CD44, CD29, CD105 and CD90, and negative for CD133, CD34 and CD36. (B) Flow cytometry also revealed that CD29, CD44, CD90 and CD105 were highly expressed and CD133, CD34 and CD36 were nearly negligible on the cells. Scale bar, 25 μm.

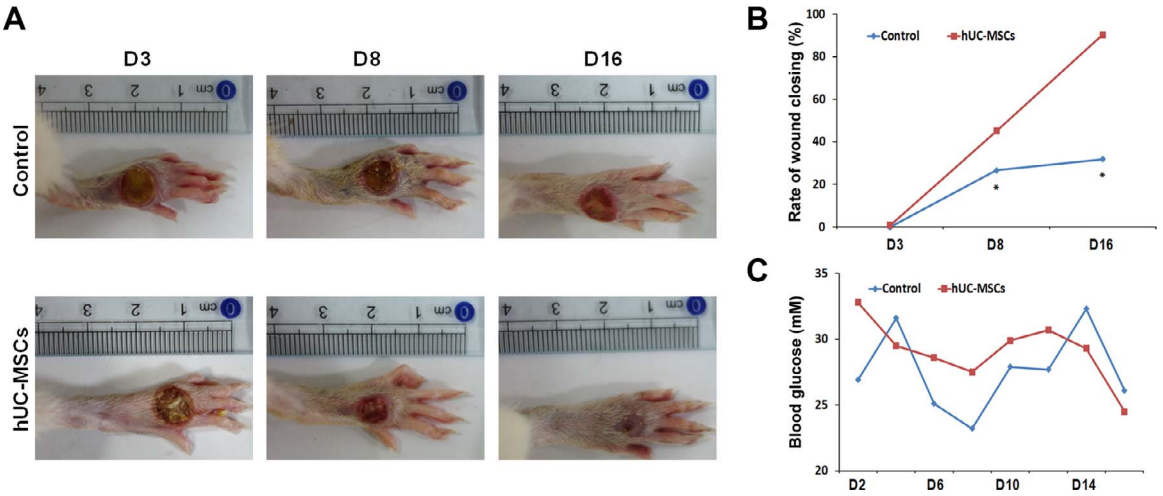

Figure 3. DFU healing and blood glucose level at different time points after treatment (A) Representative changes of DFUs in the control group and hUC-MSC treatment group at D3, D8 and D16 after treatment. (B) The rate of wound closing in DFUs in hUC-MSC-treated model rats during observation compared with control model rats at D3, D8 and D16 after injection. The ulcer area in each foot was measured from the pictures taken at each time point using Image-Pro Plus 6.0 image analysis software, and the rate of wound closing was defined as a percentage of the wound area at each time divided by D3. (C) The blood glucose levels during the entire treatment. Blood glucose level was checked at random every other day. There was no significant difference between the two groups ($P > 0.05$). Data were presented as the mean ± SD, n = 5, at each time point. $^*P < 0.05$.

compared with the control (Fig. 4B). Collagens are mainly expressed and distributed in the dermis of the skin and are closely associated with the repair of injured skin. In order to detect collagen formation, Masson trichrome staining with computer-aided morphological analysis was used, and results showed that there were more collagen tissues in the fibers in the hUC-MSC-treated rats than in the control rats, with density value of 0.31 ± 0.02 in the control group versus 0.72 ± 0.06 in the treatment group ($P < 0.05$; Fig. 4C). These data suggest that transplanted hUC-MSCs accelerate wound healing in DFU rats by promoting epithelialization, granulation tissue formation and collagen deposition.

Angiogenesis is another key factor during the wound healing; therefore, the new small blood vessels in the DFUs at D16 after treatment were evaluated by immunohistochemical staining of CD31. Dense small vessels growing widely in wound granulation tissue could be detected in the treatment group, but sparse new vessels in the DFUs were present in the control group. Compared with that in the control group, the vascular density in the hUC-MSC-

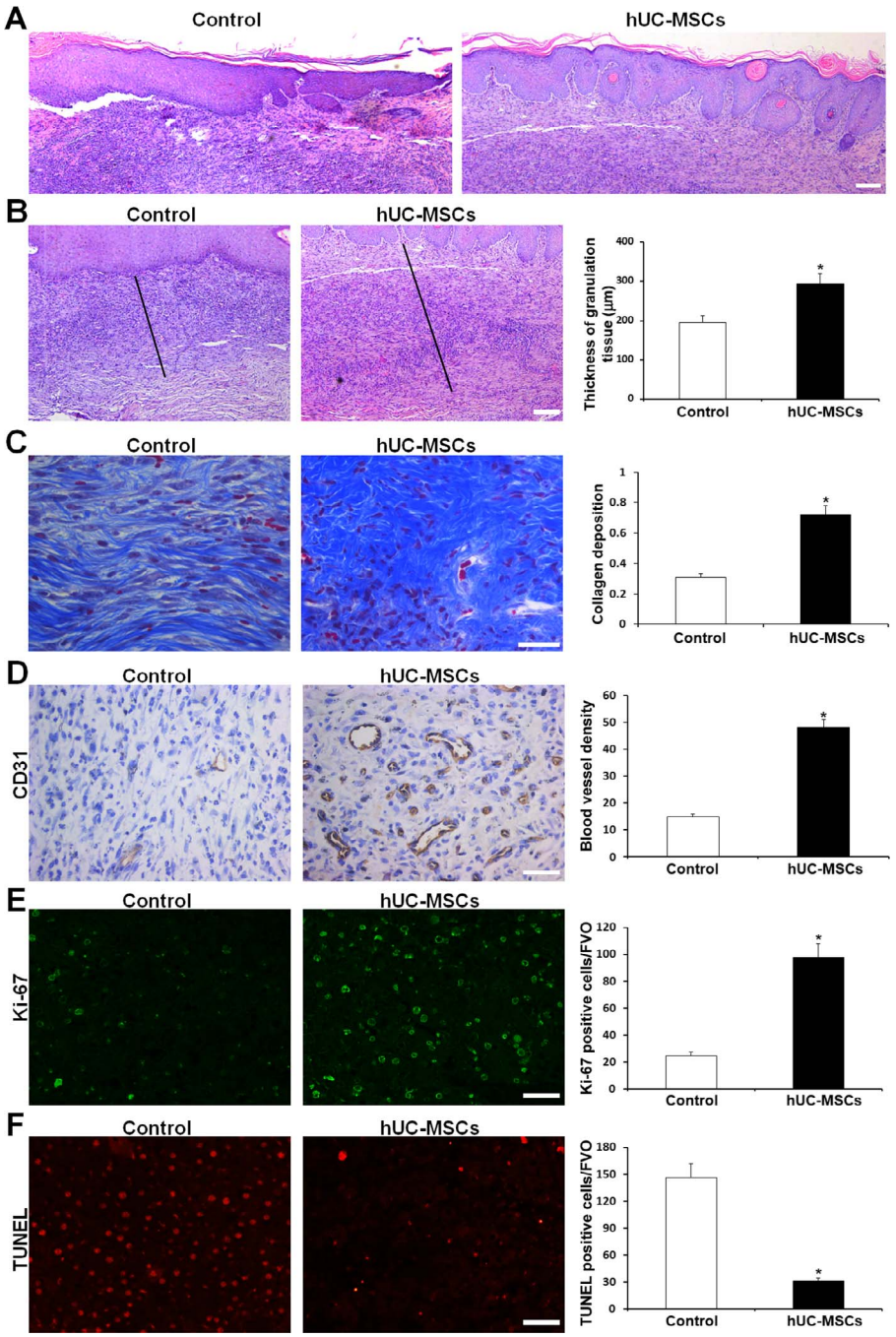

Figure 4. hUC-MSCs promoted the epithelialization and granulation, tissue regeneration, angiogenesis, cell proliferation and reduced apoptosis in DFUs at D16 after treatment (A) H&E staining showed better dermal re-epithelialization on the DFU wound beds treated with hUC-MSCs compared with the control model rats. (B) The granulation tissues in hUC-MSC treatment group were thicker than that in the control group. (C) Masson trichrome staining evidently showed more collagen deposition in hUC-MSC treatment group compared with the control group. (D) Immunohistochemical staining of CD31 showed more blood vessel structures on the wound beds in the hUC-MSC group compared with the control group. (E) Ki-67 staining revealed more positive cells in the hUC-MSC groups than that in the control group, indicating that hUC-MSC treatment promoted cell proliferation in DFUs. (F) Apoptotic cells were detected by TUNEL assays. Few apoptotic cells were detected in the hUC-MSC treatment group, suggesting that hUC-MSCs reduced the apoptosis in the process of healing. Data were presented as the mean ± SD. $^{*}P < 0.05$. Scale bar, 100 μm.

treated group was significantly higher (Fig. 4D). The situation of cellular proliferation in the wound tissues is another important element contributed to the ulcer healing; therefore, Ki-67 staining was employed to investigate whether the transplanted hUC-MSCs could promote cell proliferation in the DFUs. There were Ki-67 positive cells diffusely distributed in the basal layer of wound epidermis in the treatment group, but only a few in the control group. Compared with that in the control group, the average expression of Ki-67 in DFUs treated with hUC-MSCs was significantly higher (Fig. 4E). In addition, the situation of cell apoptosis in the DFUs was

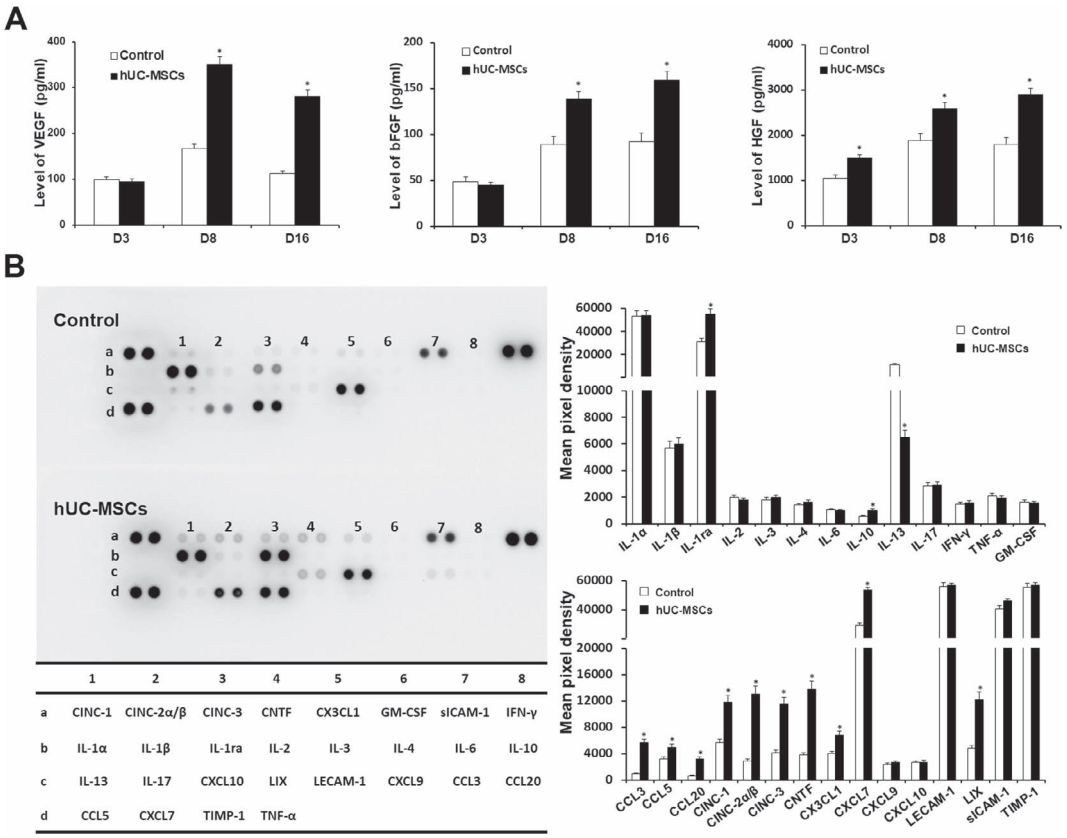

	1	2	3	4	5	6	7	8
a	CINC-1	CINC-2α/β	CINC-3	CNTF	CX3CL1	GM-CSF	sICAM-1	IFN-γ
b	IL-1α	IL-1β	IL-1ra	IL-2	IL-3	IL-4	IL-6	IL-10
c	IL-13	IL-17	CXCL10	LIX	LECAM-1	CXCL9	CCL3	CCL20
d	CCL5	CXCL7	TIMP-1	TNF-α				

Figure 5. Effect of hUC-MSC treatment on cytokines and chemokines in DFU wound beds (A) The levels of VEGF, bFGF and HGF at D3, D8 and D16 were determined by ELISA. (B) The R&D Systems Rat Cytokine Antibody Proteome Profiler Array system was employed to detect the inflammation-related cytokines and chemokines in the DFU tissues at D3 after treatment. Quantification of cytokines and chemokines, and the mean pixel density was analyzed with Image-Pro Plus 6.0. $^{*}P < 0.05$.

also evaluated by TUNEL assay. The apoptotic cells in the control group had obvious nuclear cell characteristics, which indicated that the apoptotic cells were much more than those in the hUC-MSC treatment group. Quantitative analysis showed that the apoptotic cells in the control group were increased about five folds when compared with those in the hUC-MSC treatment group (Fig. 4F). These results demonstrated that with more angiogenesis and cellular proliferation, less cellular apoptosis could be achieved in the process of the ulcer healing in the rats treated with hUC-MSCs.

Paracrine effects of hUC-MSCs in DFUs

It is generally accepted that transplanted MSCs promote tissue repair mainly through paracrine mechanisms. The levels of VEGF, bFGF and HGF were measured by ELISA. The levels of VEGF and bFGF were significantly higher in the DFUs treated with hUC-MSCs than in the control at D8 and D16, while HGF was maintained at a high level at all the three time points, which indicated that hUC-MSCs resulted in an increase in wound angiogenesis (Fig. 5A). Various cytokines and chemokines play an important role in inflammation, and many factors constitute a network, one of which is regulated by one or more other cytokines. Thus, we evaluated the levels of major cytokines and chemokines in DFUs on D3 after treatment by using proteomic analyzer array, which allowed simultaneous analysis of 28 factors in a single experiment. It was found that the levels of IL-1ra, IL-10, CCL3, CCL5, CCL20, CINC-1, CINC-2α/β, CINC-3, CNTF, CX3CL1, CXCL7 and LIX were significantly up-regulated, whereas IL-13 was significantly restrained in the treatment group compared with those in the control group ($P < 0.05$; Fig. 5B). Our data revealed that transplanted hUC-MSCs had the ability to modulate the synthesis of several cytokines and chemokines which are involved in the inflammatory process to restrain the inflammatory reaction.

Trace of the hUC-MSCs in DFU tissues after transplantation

The satisfactory healing effect prompts us to explore and trace the distribution of hUC-MSCs transplanted via femoral vein. The lentivirus expressing ZsGreen was employed to infect the hUC-MSCs, and the labeling efficiency was ~90% (Fig. 6A). The labeled hUC-MSCs were transplanted to the DFU rats via femoral vein in the same way as the previous treatment experiment. An additional 24-h period was added to detect whether the hUC-MSCs could come to the ulcers rapidly. The frozen sections of ulcer tissues were prepared at 24 h, D3, D8 and D16 after transplantation, and the distribution and intensity of ZsGreen-positive cells were detected immediately (n = 5). Other observers blind to the observational group counted the numbers of ZsGreen-positive cells and total cells in the fields, and the intensity of transplanted cells in the DFUs in this study was defined as a percentage of the number of ZsGreen-positive cells divided by the total cell number. The ZsGreen-positive cells could be detected in the DFUs 24 h after hUC-MSC transplantation with the intensity of 2.9% ± 0.2%, suggesting that transplanted cells via

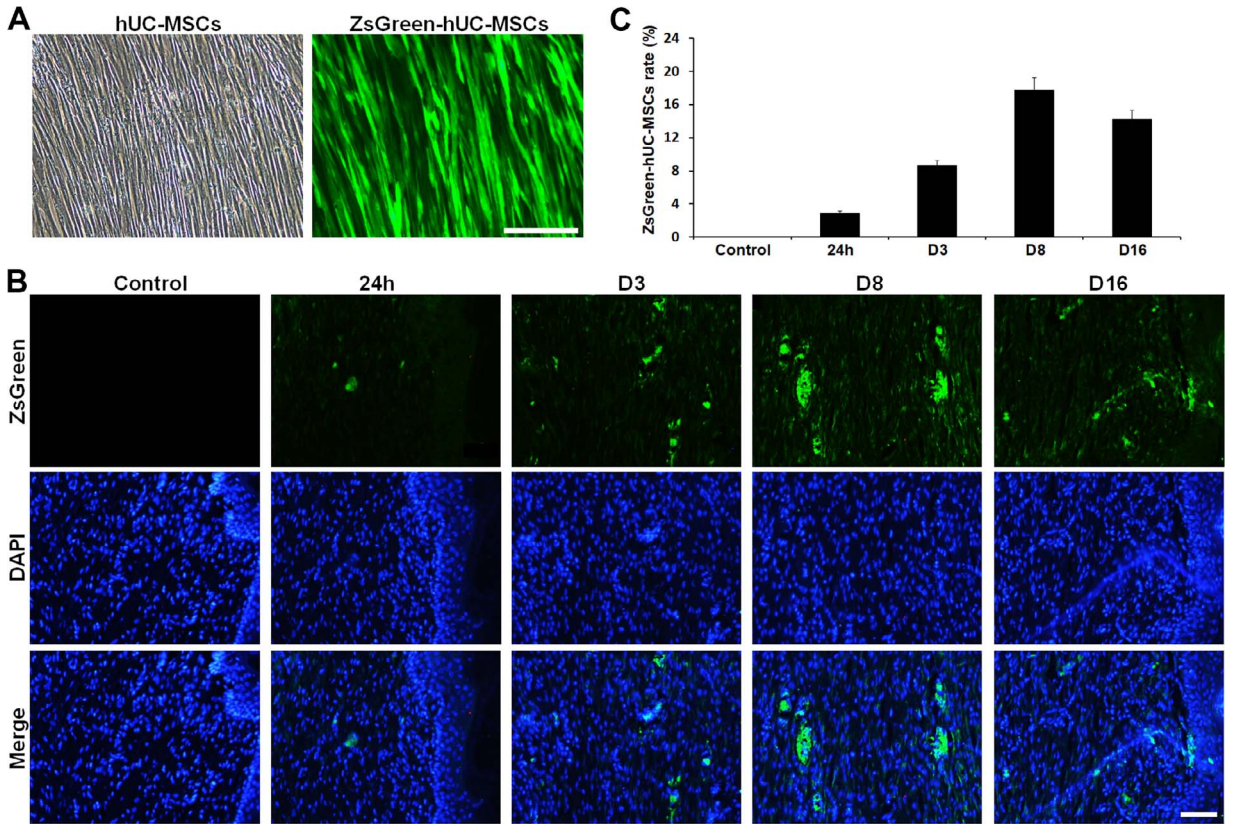

Figure 6. Trace of the hUC-MSCs in DFU tissues after transplantation (A) The hUC-MSCs were labeled with the lentivirus expressing ZsGreen and detected under bright-field and green fluorescence. (B) The images of transplanted ZsGreen-positive cells at different time points in DFU wound beds. (C) The rate of ZsGreen-positive cells at different time points. Data were presented as the mean ± SD. Scale bar, 100 μm.

femoral vein had the ability to migrate and find home to the injury skin tissues rapidly, although the quantity was not very large. In addition, the ZsGreen-positive cells could also be found at D3, D8 and D16, and their intensities were 8.6% ± 0.7%, 17.8% ± 1.4% and 14.2% ± 1.1%, respectively (Fig. 6B,C). The transplanted hUC-MSCs reached and survived in the ulcer tissues at all the time points, and the highest intensity was achieved at D8, suggesting that vein transplanted hUC-MSCs migrate to the wound area and contribute to the wound healing during the whole process.

Fate of hUC-MSCs in DFU tissues

The high rate of ZsGreen-positive cells in the DFUs prompts us to further explore the fate of transplanted hUC-MSCs. A large number of ZsGreen positive cells were found in different parts of the ulcer, especially at D8 and D16, which may indicate the multidirectional differentiation potential of hUC-MSCs *in vivo*. In order to determine whether hUC-MSCs were engrafted and differentiated into vascular structures, we further examined whether ZsGreen positive cells expressed CD31 simultaneously with frozen sections of ulcer tissue at D16 after transplantation. ZsGreen and CD31 double positive cells were detected in newly formed capillaries, indicating that the transplanted hUC-MSCs were spontaneously differentiated into endothelial phenotype, while no ZsGreen positive cells were found in the control group, indicating the specificity of ZsGreen immunostaining (Fig. 7A). Because of the presence of ZsGreen positive cells in the newly formed dermis and epidermis, further co-staining of epithelial keratin and ZsGreen was performed in the wound area at D16 to determine whether hUC-MSCs have the potential of epithelial differentiation. In the treatment group, the transplanted ZsGreen positive cells combined with dermal structure and expressed pan-cytokeratin positive signals, while in the control group, no ZsGreen positive cells were found (Fig. 7B). These findings indicated that ZsGreen-positive hUC-MSCs were incorporated and differentiated into regenerated epidermal and vascular structures to enhance the wound epithelialization and healing.

Discussion

The global prevalence of diabetes has risen dramatically, which is expected to continue to impose a huge financial burden. In the lifetime of diabetic patients, 12% to 25% suffer from diabetic complications [17]. Foot ulcer has a significant impact on the quality of life of patients. Foot ulcer has negative effects such as pain, social isolation, physical morbidity, work ability limitation and mental health [18]. Successful wound healing is a dynamic and complex process, including a series of coordinated events: inflammation, cell migration, proliferation, differentiation, angiogenesis, fibrosis, re-epithelialization and tissue remodeling [19]. Some studies have confirmed that wound healing may be interfered by infection, necrosis and excessive inflammatory factors. And if the wound continues to inflame, it will cause a persistent state of nonunion [20,21]. DFU is an outcome of complicated amalgam of various risk factors such as peripheral neuropathy, peripheral vascular disease, foot deformities, arterial insufficiency, trauma and impaired resistance to infection

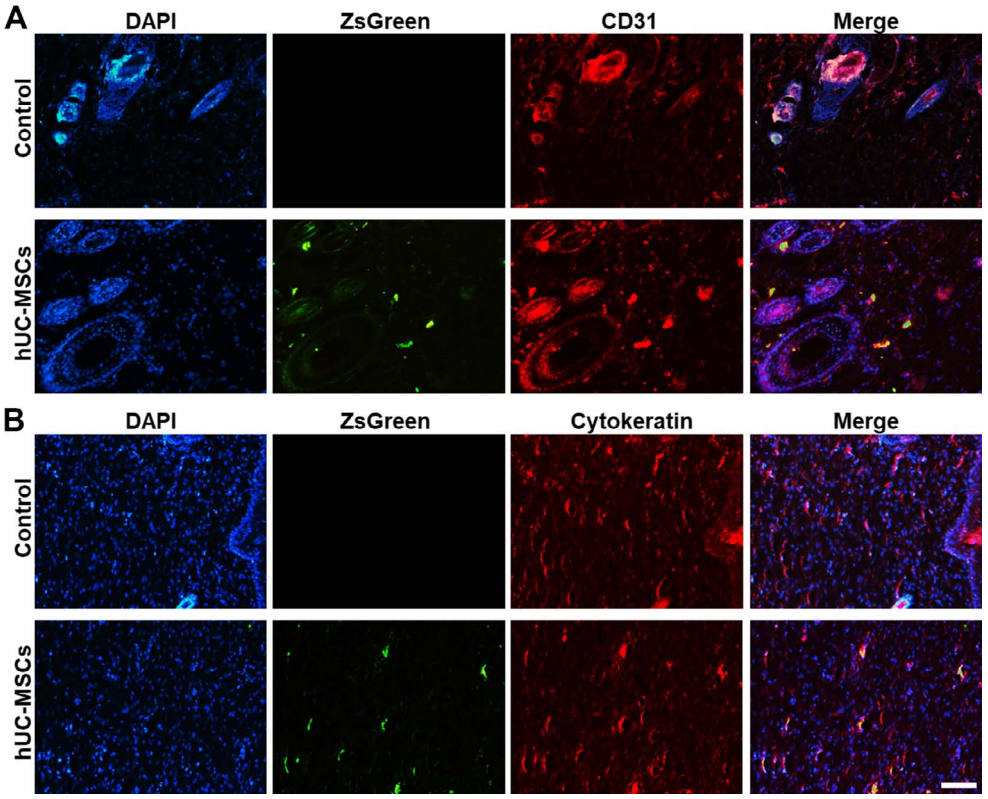

Figure 7. Fate of hUC-MSCs in DFU tissues (A) Frozen sections of DFU tissues at D16 in hUC-MSC treatment group showed the ZsGreen-positive cells were concomitant with the staining of CD31, which revealed that transplanted ZsGreen-hUC-MSCs were differentiated into endothelial cells expressing CD31 and incorporated into the vascular structures. (B) Frozen sections of DFU tissues at D16 in hUC-MSC treatment group showed the co-staining of cytokeratin and ZsGreen, which revealed that transplanted ZsGreen-hUC-MSCs were differentiated into epithelial cells expressing cytokeratin. Scale bar, 100 μm.

[22,23]. These factors may damage wound healing in DFUs and prolong one or more stages of inflammation, proliferation and remodeling [24]. DFUs still remain an important challenge since the available therapies have limited efficacy and some of the novel therapeutic approaches, which include the recombinant growth factors, are very expensive [25]. Most of them are directed against a single etiological factor, whereas a variety of factors lead to the formation of DFUs. The ideal treatment of DFUs should have the synergistic effects of anti-inflammation, granulation tissue formation, cell proliferation and angiogenesis.

UC-MSCs may be a good choice for the treatment of chronic trauma such as DFU. It was reported that MSCs are ideal candidates for tissue repair [12]. Previous studies have shown that UC-MSCs can effectively repair acute kidney injury and liver injury caused by ischemia-reperfusion injury [26–28]. In addition, hUC-MSCs have good proliferation and differentiation ability and low immune resistance, which are considered as an alternative source of stem cells for cutaneous regeneration in patients with DFUs [29,30]. In present study, full-thickness foot dorsal skin wounds in streptozotocin injected rats were employed to mimic DFUs and transplanted with the hUC-MSCs via femoral vein. Transplanted hUC-MSCs labeled by ZsGreen were proved to be able to migrate and find home to the wound tissues and locate in the wound edge and wound base. But the mechanism responsible for the homing of hUC-MSCs to wounds is not well understood and it may involve the complex interplay of adhesion molecules, chemokines and extracellular matrix proteases [31]. Compared with the control group, the ulcer size in the hUC-MSC treatment group was decreased significantly, and the recovery was gradual and obvious. We also found that transplanted hUC-MSCs promoted re-epithelialization and granulation tissue formation, significantly enhanced angiogenesis and cell proliferation, and decreased cell apoptosis. Simultaneously, the transplanted hUC-MSCs increased the secretion of growth factors (VEGF, bFGF and HGF) and restrained the inflammation reaction. It has been recognized that wound healing may be interfered by infection, necrosis and excessive inflammatory factors [21,29]. Our results showed that hUC-MSC transplantation significantly increased the production of the anti-inflammatory cytokines such as IL-10 and the chemokines such as CCL, CINC and CX3CL, which are main participants in the anti-inflammatory cytokine profile of hUC-MSCs.

The blood supply is the key to wound healing. Angiogenesis involves a variety of coordinated events, including the degradation of extracellular matrix around the parent vessel, migration and proliferation of endothelial cells and parietal cells to assemble new vessels, lumen formation, and the construction of mural cell layers of the vessel wall with associated pericytes and smooth muscle cells [32]. Paracrine effect is considered to be the main mechanism for the role of MSCs in tissue repair [33,34]. Some MSC-secreted paracrine growth factors conducive to angiogenesis such as VEGF, bFGF and HGF have been demonstrated to promote the neovascularization of injured tissues [35,36]. Some study also indicated that MSCs are able to improve tissue vascularity by promoting endothelial cell sprouting through soluble factor secretion [37]. Our data also revealed that

hUC-MSCs increased the levels of VEGF, bFGF and HGF in DFU wound beds and promoted wound angiogenesis. Furthermore, we speculated that hUC-MSCs may accelerate the DFU wound healing by paracrine effects to increase wound angiogenesis.

Collagen, as a structurally and functionally pivotal molecule which builds a scaffold in the connective tissue, is also involved in every stage of wound healing [38]. Our results showed that hUC-MSCs could increase the collagen deposition in the granulation tissues of DFU wound beds. Granulation tissue is also essential to wound healing, as it is formed on the surface of wounds to protect and provide nutrition to the wounds. It consists of fibroblasts, new capillaries, and infiltrated inflammatory cells. The granulation tissue was thicker and almost completely re-epithelialized, the cell proliferation was increased, and the cell apoptosis was decreased in the hUC-MSC group. All these advantages in the DFU wound beds of the hUC-MSC treatment group may also be due to the paracrine action and inflammation regulation of hUC-MSCs.

In order to further explore the potential mechanism by which hUC-MSCs promote wound healing, we applied hUC-MSCs expressing ZsGreen to wound healing to determine whether hUC-MSCs engrafted into wounds could differentiate along multiple lineages of tissue regeneration in a specific microenvironment. Some studies have shown that human MSCs have the potential of epithelial differentiation under appropriate culture conditions [39]. Our data showed that ZsGreen-positive hUC-MSCs appeared to coexist with the staining of the first epithelial-specific structural protein pan-cytokeratin *in vivo*, suggesting that ZsGreen-positive hUC-MSCs spontaneously differentiated into epithelial cells. In addition, our results also revealed that transplanted ZsGreen-positive cells co-expressed CD31, a phenotypic marker of vascular endothelium. These findings further supported the fact that intravenous transplanted hUC-MSCs can migrate to wound tissue and differentiate into endothelial cells *in situ*, contributing to the formation of neovascularization. Our study is consistent with previous studies reporting that human adipose-derived stem cells can differentiate into endothelial cells and improve postnatal neovascularization, demonstrating that human MSCs have similar characteristics [40].

In this study, we demonstrated an important component of wound healing effect induced by hUC-MSCs, which may be a particularly promising treatment for chronic non-healing wounds, such as DFUs. Our research showed that transplanted hUC-MSCs could migrate and find home to the wound tissues, creating a biological microenvironment to accelerate healing. Paracrine action and transdifferentiation are the potential mechanisms for the role of hUC-MSCs in DFU wound bed repair. Previously, we used human adipose-derived stem cells to treat DFUs in rat models and achieved good results [41]. If it was widely used in clinic, the demand for fat would be quite large; however, the source of fat is sometimes limited. By contrast, the umbilical cord is easy to obtain because almost all the delivery women in China often discard it. In this study, we demonstrated that human umbilical cord stem cells have almost the same efficacy as adipose-derived stem cells in the treatment of DFU model, which provides a premise for the large-scale future use in clinic. The combined use of hUC-MSCs with the existing treatment in chronic non-healing wounds may have advantages over the current single treatment. However, the mechanisms underlying these actions remain to be elucidated. Because of the short period of treatment, the potential negative side effects were not assessed in this study, and in the future long-term systemic effects of stem cell therapy should be established and the safety of stem cell therapy should also be addressed.

In conclusion, transplanted hUC-MSCs via vein improve wound healing in the DFU model of rats through paracrine action and transdifferentiation, and transplantation of UC-MSCs may provide a new strategy for the treatment of DFUs.

Funding

This work was supported in part by the grants from the Natural Science Foundation of Jiangsu Province of China (No. BK20180946), the Natural Science Foundation of Nantong City (No. MS12018068), and the Science Foundation of China Postdoctoral (No. 2019M651928).

References

1. Deng W, Qiu S, Yang G, Chen B. Exenatide once weekly injection for the treatment of type 2 diabetes in Chinese patients: current perspectives. *Ther Clin Risk Manag* 2015, 11: 1153–1162.
2. Skrepnek GH, Mills JL Sr, Armstrong DG. A diabetic emergency one million feet long: disparities and burdens of illness among diabetic foot ulcer cases within emergency departments in the United States, 2006–2010. *PLoS One* 2015, 10: 8.
3. Gadelkarim M, Abushouk AI, Ghanem E, Hamaad AM, Saad AM, Abdel-Daim MM. Adipose-derived stem cells: effectiveness and advances in delivery in diabetic wound healing. *Biomed Pharmacother* 2018, 107: 625–633.
4. Nirantharakumar K, Saeed M, Wilson I, Marshall T, Coleman JJ. In-hospital mortality and length of stay in patients with diabetes having foot disease. *J Diabetes Complications* 2013, 27: 454–458.
5. Yoo HS, Yi T, Cho YK, Kim WC, Song SU, Jeon MS. Mesenchymal stem cell lines isolated by different isolation methods show variations in the regulation of graft-versus-host disease. *Immune Netw* 2013, 13: 133–140.
6. Sun L, Wang D, Liang J, Zhang H, Feng X, Wang H, Hua B, *et al*. Umbilical cord mesenchymal stem cell transplantation in severe and refractory systemic lupus erythematosus. *Arthritis Rheum* 2010, 62: 2467–2475.
7. Wang X, Wang Y, Gou W, Lu Q, Peng J, Lu S. Role of mesenchymal stem cells in bone regeneration and fracture repair: a review. *Int Orthop* 2013, 37: 2491–2498.
8. Çil N, Oğuz EO, Mete E, Çetinkaya A, Mete GA. Effects of umbilical cord blood stem cells on healing factors for diabetic foot injuries. *Biotech Histochem* 2017, 92: 15–28.
9. Wu Y, Chen L, Scott PG, Tredget EE. Mesenchymal stem cells enhance wound healing through differentiation and angiogenesis. *Stem Cells* 2007, 25: 2648–2659.
10. Weissman IL. Stem cells: units of development, units of regeneration, and units in evolution. *Cell* 2000, 100: 157–168.
11. Batsali AK, Kastrinaki MC, Papadaki HA, Pontikoglou C. Mesenchymal stem cells derived from Wharton's jelly of the umbilical cord: biological properties and emerging clinical applications. *Curr Stem Cell Res Ther* 2013, 8: 144–155.
12. Fathke C, Wilson L, Hutter J, Kapoor V, Smith A, Hocking A, Isik F. Contribution of bone marrow-derived cells to skin: collagen deposition and wound repair. *Stem Cells* 2004, 22: 812–822.
13. Wang HS, Hung SC, Peng ST, Huang CC, Wei HM, Guo YJ, Fu YS, *et al*. Mesenchymal stem cells in the Wharton's jelly of the human umbilical cord. *Stem Cells* 2004, 22: 1330–1337.
14. Lanci A, Merlo B, Mariella J, Castagnetti C, Iacono E. Heterologous Wharton's jelly derived mesenchymal stem cells application on a large chronic skin wound in a 6-month-old filly. *Front Vet Sci* 2019, 6: 9.
15. La Rocca G, Anzalone R, Corrao S, Magno F, Loria T, Lo Iacono M, Di Stefano A, *et al*. Isolation and characterization of Oct-4+/HLA-G+ mesenchymal stem cells from human umbilical cord matrix: differentiation potential and detection of new markers. *Histochem Cell Biol* 2009, 131: 267–282.

16. Zhang XY, La Russa VF, Reiser J. Transduction of bone-marrow-derived mesenchymal stem cells by using lentivirus vectors pseudotyped with modified RD114 envelope glycoproteins. *J Virol* 2004, 78: 1219–1229.
17. Brem H, Sheehan P, Rosenberg HJ, Schneider JS, Boulton AJ. Evidence-based protocol for diabetic foot ulcers. *Plast Reconstr Surg* 2006, 117: 193S–209S.
18. Herber OR, Schnepp W, Rieger MA. A systematic review on the impact of leg ulceration on patients' quality of life. *Health Qual Life Outcomes* 2007, 5: 44.
19. Maxson S, Lopez EA, Yoo D, Danilkovitch-Miagkova A, Leroux MA. Concise review: role of mesenchymal stem cells in wound repair. *Stem Cells Transl Med* 2012, 1: 142–149.
20. Choi H, Lee RH, Bazhanov N, Oh JY, Prockop DJ. Anti-inflammatory protein TSG-6 secreted by activated MSCs attenuates zymosan-induced mouse peritonitis by decreasing TLR2/NF-kappaB signaling in resident macrophages. *Blood* 2011, 118: 330–338.
21. Krasnodembskaya A, Song Y, Fang X, Gupta N, Serikov V, Lee JW, Matthay MA. Antibacterial effect of human mesenchymal stem cells is mediated in part from secretion of the antimicrobial peptide LL-37. *Stem Cells* 2010, 28: 2229–2238.
22. Pereira SG, Moura J, Carvalho E, Empadinhas N. Microbiota of chronic diabetic wounds: ecology, impact, and potential for innovative treatment strategies. *Front Microbiol* 2017, 8: 1791.
23. Khanolkar MP, Bain SC, Stephens JW. The diabetic foot. *QJM* 2008, 101: 685–695.
24. Falanga V. Wound healing and its impairment in the diabetic foot. *Lancet* 2005, 366: 1736–1743.
25. Saaristo A, Tammela T, Farkkilā A, Kärkkäinen M, Suominen E, Yla-Herttuala S, Alitalo K. Vascular endothelial growth factor-C accelerates diabetic wound healing. *Am J Pathol* 2006, 169: 1080–1087.
26. Cao H, Qian H, Xu W, Zhu W, Zhang X, Chen Y, Wang M, *et al*. Mesenchymal stem cells derived from human umbilical cord ameliorate ischemia/reperfusion-induced acute renal failure in rats. *Biotechnol Lett* 2010, 32: 725–732.
27. Tögel F, Weiss K, Yang Y, Hu Z, Zhang P, Westenfelder C. Vasculotropic, paracrine actions of infused mesenchymal stem cells are important to the recovery from acute kidney injury. *Am J Physiol Renal Physiol* 2007, 292: F1626–F1635.
28. Chen Y, Qian H, Zhu W, Zhang X, Yan Y, Ye S, Peng X, *et al*. Hepatocyte growth factor modification promotes the amelioration effects of human umbilical cord mesenchymal stem cells on rat acute kidney injury. *Stem Cells Dev* 2011, 20: 103–113.
29. Chen K, Wang D, Du WT, Han ZB, Ren H, Chi Y, Yang SG, *et al*. Human umbilical cord mesenchymal stem cells hUC-MSCs exert immunosuppressive activities through a PGE2-dependent mechanism. *Clin Immunol* 2010, 135: 448–458.
30. Li T, Yan Y, Wang B, Qian H, Zhang X, Shen L, Wang M, *et al*. Exosomes derived from human umbilical cord mesenchymal stem cells alleviate liver fibrosis. *Stem Cells Dev* 2013, 22: 845–854.
31. Karp JM, Leng Teo GS. Mesenchymal stem cell homing: the devil is in the details. *Cell Stem Cell* 2009, 4: 206–216.
32. Yoo SY, Kwon SM. Angiogenesis and its therapeutic opportunities. *Mediators Inflamm* 2013, 2013: 127170.
33. Salem HK, Thiemermann C. Mesenchymal stromal cells: current understanding and clinical status. *Stem Cells* 2010, 28: 585–596.
34. Camussi G, Deregibus MC, Tetta C. Paracrine/endocrine mechanism of stem cells on kidney repair: role of microvesicle mediated transfer of genetic information. *Curr Opin Nephrol Hypertens* 2010, 19: 7–12.
35. Wang M, Crisostomo PR, Herring C, Meldrum KK, Meldrum DR. Human progenitor cells from bone marrow or adipose tissue produce VEGF, HGF, and IGF-I in response to TNF by a p38 MAPK-dependent mechanism. *Am J Physiol Regul Integr Comp Physiol* 2006, 291: R880–R884.
36. Wang Y, Wang M, Abarbanell AM, Weil BR, Herrmann JL, Tan J, Novotny NM, *et al*. MEK mediates the novel cross talk between TNFR2 and TGF-EGFR in enhancing vascular endothelial growth factor (VEGF) secretion from human mesenchymal stem cells. *Surgery* 2009, 146: 198–205.
37. Johansson U, Rasmusson I, Niclou SP, Forslund N, Gustavsson L, Nilsson B, Korsgren O, *et al*. Formation of composite endothelial cell-mesenchymal stem cell islets: a novel approach to promote islet revascularization. *Diabetes* 2008, 57: 2393–2401.
38. Iyyam Pillai S, Palsamy P, Subramanian S, Kandaswamy M. Wound healing properties of Indian propolis studied on excision wound-induced rats. *Pharm Biol* 2010, 48: 1198–1206.
39. Brzoska M, Geiger H, Gauer S, Baer P. Epithelial differentiation of human adipose tissue-derived adult stem cells. *Biochem Biophys Res Commun* 2005, 330: 142–150.
40. Cao Y, Sun Z, Liao L, Meng Y, Han Q, Zhao RC. Human adipose tissue-derived stem cells differentiate into endothelial cells in vitro and improve postnatal neovascularization in vivo. *Biochem Biophys Res Commun* 2005, 332: 370–379.
41. Shi R, Jin Y, Cao C, Han S, Shao X, Meng L, Cheng J, *et al*. Localization of human adipose-derived stem cells and their effect in repair of diabetic foot ulcers in rats. *Stem Cell Res Ther* 2016, 7: 155.